Old Dominion University
ODU Digital Commons

Chemistry & Biochemistry Faculty Publications   Chemistry & Biochemistry

2015

Molecular Level Characterization of Diatom-Associated Biopolymers that Bind 234Th, ^{233}PA, ^{210}Pb, and 7Be in Seawater: A Case Study With Phaeodactylum tricornutum

Chia-Ying Chuang

Peter H. Santschi

Chen Xu

Yuelu Jiang

Yi-Fang Ho

See next page for additional authors

Follow this and additional works at: https://digitalcommons.odu.edu/chemistry_fac_pubs

🌐 Part of the Environmental Sciences Commons, and the Geology Commons

Authors

Chia-Ying Chuang, Peter H. Santschi, Chen Xu, Yuelu Jiang, Yi-Fang Ho, and Patrick G. Hatcher

Correspondence to:
C.-Y. Chuang,
anderin.chuang@gmail.com

Molecular level characterization of diatom-associated biopolymers that bind ^{234}Th, ^{233}Pa, ^{210}Pb, and ^{7}Be in seawater: A case study with *Phaeodactylum tricornutum*

Chia-Ying Chuang[1,2], Peter H. Santschi[1,2], Chen Xu[1,2], Yuelu Jiang[3,4], Yi-Fang Ho[2], Antonietta Quigg[1,2,3], Laodong Guo[5], Patrick G. Hatcher[6], Marin Ayranov[7], and Dorothea Schumann[8]

[1]Department of Oceanography, Texas A&M University, College Station, Texas, USA, [2]Department of Marine Sciences, Texas A&M University, Galveston, Texas, USA, [3]Department of Marine Biology, Texas A&M University, Galveston, Texas, USA, [4]Institute of Ocean Science and Technology, Graduate School at Shenzhen, Tsinghua University, Shenzhen, China, [5]School of Freshwater Sciences, University of Wisconsin-Milwaukee, Milwaukee, Wisconsin, USA, [6]Department of Chemistry and Biochemistry, Old Dominion University, Norfolk, Virginia, USA, [7]European Commission, DG-Energy, Luxembourg, [8]Paul Scherrer Institute, Villigen, Switzerland

Abstract In order to investigate the importance of biogenic silica associated biopolymers on the scavenging of radionuclides, the diatom *Phaeodactylum tricornutum* was incubated together with the radionuclides ^{234}Th, ^{233}Pa, ^{210}Pb, and ^{7}Be during their growth phase. Normalized affinity coefficients were determined for the radionuclides bound with different organic compound classes (i.e., proteins, total carbohydrates, uronic acids) in extracellular (nonattached and attached exopolymeric substances), intracellular (ethylene diamine tetraacetic acid and sodium dodecyl sulfate extractable), and frustule embedded biopolymeric fractions (BF). Results indicated that radionuclides were mostly concentrated in frustule BF. Among three measured organic components, Uronic acids showed the strongest affinities to all tested radionuclides. Confirmed by spectrophotometry and two-dimensional heteronuclear single quantum coherence-nuclear magnetic resonance analyses, the frustule BF were mainly composed of carboxyl-rich, aliphatic-phosphoproteins, which were likely responsible for the strong binding of many of the radionuclides. Results from this study provide evidence for selective absorption of radionuclides with different kinds of diatom-associated biopolymers acting in concert rather than as a single compound. This clearly indicates the importance of these diatom-related biopolymers, especially frustule biopolymers, in the scavenging and fractionation of radionuclides used as particle tracers in the ocean.

1. Introduction

Due to their particle reactive nature, Th, Pa, Pb, and Be radionuclides are removed from the water column by "scavenging," i.e., adsorption on particles and colloids, and subsequent removal with aggregating particles to the sediments. Differences in particle reactivity lead to different distributions and disequilibrium patterns of mother and daughter radionuclides in the water column. Oceanographers have exploited the reactions of these particle-reactive radionuclides to derive quantitative information on sources and fluxes of particles [*Anderson et al.*, 1983; *Bacon et al.*, 1976], carbon [*Friedrich and Rutgers van der Loeff*, 2002], and other chemical species [*Cochran et al.*, 1983; *Li et al.*, 1979; *Santschi et al.*, 1980] as well as their residence times [*Santschi*, 1984] in the present and past ocean. However, the molecular mechanisms of tracer applications to marine particle cycling remain poorly understood [*Guo et al.*, 2002a; *Li*, 2005; *Santschi et al.*, 2006]. The cumulative evidence from the analysis of data sets from field and laboratory studies showed specific particulate organic biopolymers that were demonstrated to be responsible for the binding of radionuclides due to their different metal-binding propensities. Among these four selected radionuclides, with the exception of Pb (which has intermediate properties), all others have hard (A type) metal ion characteristics preferring to bind to O (over N or S). For example, uronic acid content has been used as a good proxy to predict the Th flux [*Guo et al.*, 2002b; *Santschi et al.*, 2003; *Xu et al.*, 2011]. More recently, hydroxamate siderophoric moieties were found to be important for the binding of Pa and Po to sinking particles [*Chuang et al.*, 2013], as well as for the binding of Th and Pa to marine colloids [*Chuang et al.*, 2015]. Moreover, results from radiotracer experiments showed that biogenic silica (BSi) alone is not a strong binding agent for different radionuclides, but silica-associated biopolymers are [*Chuang et al.*, 2014].

BSi from diatom frustules is preserved to a significant extent in the sedimentary record and has been studied extensively from biological, paleooceanographic, and geochemical perspectives. Its biogenic sediment burial rate in marine sediments is second only to that of calcium carbonate. Responsible for as much as 45–48% of the primary production occurring in the surface ocean [e.g., *Nelson et al.*, 1995], diatoms contribute a great percentage to the organic-carbon flux exported from the euphotic zone to the deep ocean [*Buesseler*, 1998; *Richardson and Jackson*, 2007]. The nanostructure of diatom frustules is controlled by proteins acting as biocatalysts, e.g., biosilica-associated peptides (silaffins), which act as templates for in vitro silica formation from a silicic acid solution [*Kröger et al.*, 1999; *Kröger et al.*, 2002]. Frustule proteins have been identified from both pennate and centric diatoms, consisting of several types of proteins including frustulins, pleuralins, silaffins, and cingulins [*Kröger and Poulsen*, 2008; *Kröger et al.*, 1999; *Kröger et al.*, 2002]. According to *Kröger and Poulsen* [2008], silaffins are phosphoproteins that become solubilized upon dissolution of the diatom silica under relatively mild conditions using an acidified ammonium fluoride solution (10 mol L^{-1} NH$_4$F pH 4–5). This solubilization distinguishes silaffins from pleuralins, as the latter can only be solubilized by using anhydrous hydrofluoric acid (HF), which not only leads to the removal of silica but also to deglycosylation and dephosphorylation [*Kröger and Poulsen*, 2008]. Cingulins are proteins associated with the girdle band region of the diatom frustule and are endowed with silica-forming and silica-templating activity [*Scheffel et al.*, 2011]. Because the silaffin polyamines contain multiple phosphate groups, they can not only strongly bind to the silanol (Si-OH) groups but also assemble metal nanoparticles. Thus, the templating biomolecules have also been useful in nanotechnology, as in the manufacturing of magnesium oxide (MgO), titanium dioxide (TiO$_2$), barium titanate (BaTiO$_3$), and other materials [*Das and Marsili*, 2011; *Kröger and Poulsen*, 2008].

Our previous studies have shown that exopolymeric substances (EPS) and frustule-embedded biomolecules in diatom cells are responsible for enhanced sorption and scavenging rather than the silica shell itself [*Chuang et al.*, 2014]. The aim of this present study is to further assess the molecular nature of the carrier biopolymer compounds for ^{234}Th, ^{233}Pa, ^{210}Pb, and ^{7}Be radionuclides, selected among the different biopolymeric fractions (BF) in the diatom cell. Furthermore, major molecular structures of selective carrier biopolymer compounds were revealed using advanced noninvasive NMR techniques. Experiments intended to differentiate uptake to various associated biopolymers by incubating radionuclides during the growth of the diatoms. Fractions were separated after diatom cultures had reached stationary phase. Fractions included extracellular (nonattached and attached EPS), frustules, and intracellular biopolymers from cell lysis (ethylene diamine tetraacetic acid (EDTA) and sodium dodecyl sulfate (SDS) extracts). Nonattached and attached exopolymeric substances (NAEPS and AEPS) are here referred to as biopolymers that are dissolved in the medium and those attached on the diatom frustules, respectively. Carrier biomolecules were subsequently separated and identified at the molecular level by applying two-dimensional heteronuclear single quantum coherence-nuclear magnetic resonance (2-D HSQC-NMR) techniques to further reveal the structure and possible binding mechanisms of the carrier phases for different radionuclides.

2. Materials and Methods

2.1. Radiolabeled Diatom Cultures

Natural seawater with a salinity of 35, collected from the Gulf of Mexico, was sequentially filtered through a 0.2 μm polycarbonate cartridge and ultrafiltered with a 1000 amu cutoff membrane to remove particulate and colloidal organic matter [*Guo et al.*, 1995; *Roberts et al.*, 2009]. The <1000 amu ultrafiltrate fraction was then used for later experiments. The ^{234}Th tracer was milked and purified from a ^{238}U solution [*Alvarado Quiroz et al.*, 2006; *Quigley et al.*, 2002]; ^{233}Pa, in equilibrium with ^{237}Np, was obtained from Pacific Northwest National Laboratory; ^{210}Pb, in 1 mol L^{-1} nitric acid (HNO$_3$), was purchased from Eckert & Ziegler Isotope Products, and the ^{7}Be tracer solution (in 0.1 mol L^{-1} hydrochloric acid, HCl) was manufactured at the Paul Scherrer Institute, Switzerland [*Schumann et al.*, 2013].

Autoclaved f/2 media (50 ml) were added to preconditioned clear polyethylene containers, and then ~10 to 15 Bq of each radionuclide tracer (^{234}Th, ^{233}Pa, ^{210}Pb, and ^{7}Be) was added. In each radiolabeled medium, 1 ml of laboratory axenic culture, *Phaeodactylum tricornutum* (UTEX 646), was then added and incubated at a temperature of 19 ± 1°C with a light:dark cycle of 14 h:10 h under an irradiance of 100 μmol quanta m^{-2} s^{-1}. Incubation experiments were carried out in duplicate. The growth status of *P. tricornutum* was monitored by changes in optical density at 750 nm (OD$_{750}$) in a parallel nonlabeled culture. When *P. tricornutum* reached
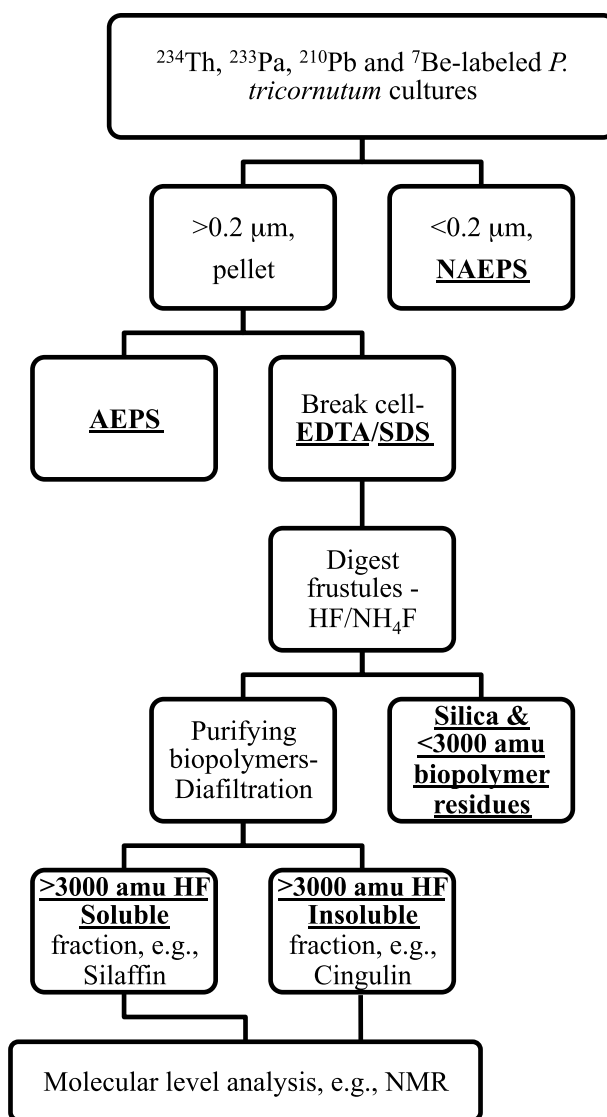
Figure 1. Scheme of chemical separation of individual biopolymeric fractions, including extracellular (NAEPS and AEPS), intracellular (EDTA and SDS extractable), and frustule embedded (>3000 amu HF soluble, >3000 amu HF insoluble, and <3000 amu), responsible for binding of different radionuclides, from radiolabeled diatom incubations.

the stationary phase observed by its OD_{750}, cells were harvested for further extraction and analyses. The total incubation time was 35 days.

2.2. Exopolymeric Substance (AEPS and NAEPS) Extraction

AEPS and NAEPS extractions were performed following the procedures described in *Chuang et al.* [2014, 2015]. Briefly, for NAEPS, laboratory cultures were centrifuged (2694 g, 30 min) and filtered (0.2 μm). The filtrate was desalted via diafiltration with a 1000 amu cutoff cross-flow ultrafiltration membrane, followed by freeze drying for later use. For the AEPS extraction, diatom cells were collected after centrifugation from the previous step. Then, the pellet was soaked with $0.5 \, \mathrm{mol \, L^{-1}}$ sodium chloride (NaCl) solution for 10 min, followed by centrifugation at 2000 g for 15 min to remove the medium and weakly bound organic material on the cells. The pellet was then resuspended in a fresh 100 ml, $0.5 \, \mathrm{mol \, L^{-1}}$ NaCl solution and stirred gently overnight at 4°C. The resuspended particle solution was ultracentrifuged at 12,000 g (30 min, 4°C), and the supernatant was then filtered through a 0.2 μm polycarbonate membrane. The filtrate was further desalted via diafiltration with a 1000 amu cutoff ultrafiltration membrane and subsequently freeze dried for later use.

2.3. Intracellular and Frustule BF Extraction

The chemical separation scheme to individual BF responsible for binding different radionuclides is given in

Figure 1, with procedures for frustule biopolymers extraction adapted from *Scheffel et al.* [2011]. Briefly, the clean diatom cells from the previous AEPS extraction step were resuspended in 10 ml, $100 \, \mathrm{m \, mol \, L^{-1}}$ EDTA (pH 8.0) at 4°C overnight. EDTA solution was used to extract the intracellular material after cell lysis. The supernatant was collected after centrifuging at 3000 g for 10 min, defined as EDTA extractable BF. Subsequently, the pellet was placed in 10 ml, 1% SDS in $10 \, \mathrm{m \, mol \, L^{-1}}$ Tris (pH 6.8) solution and heated at 95°C for 1 h. The resulting frustules were collected by centrifugation (2500 g, 10 min), washed with 10 ml milli-Q water 3 times, and then were freeze dried for later use. The supernatant from this step was collected and defined as SDS extractable BF, mostly composed of soluble cell-membrane-associated materials. These two fractions represent intracellular biopolymers lysed after cell breakage.

HF digestion was applied to help extract the diatom frustule biopolymers. HF is a nonoxidizing acid commonly used to convert SiO_2 to volatile SiF_4 during wet digestion [*Scheffel et al.*, 2011; *Šulcek and Povondra*, 1989]. Hence, frustule biopolymers could be separated from the digested solution by a 3 kDa cutoff

membrane. However, high-concentration HF would also liberate A type metal radionuclides (Th, Pa, and Be in this study) from any complex by frustule biopolymers [e.g., *Burnett et al.*, 1997]. Furthermore, deglycosylation might also have occurred during a HF digestion [*Mort and Lamport*, 1977]. Therefore, the <3000 amu fraction represents the sum of silica frustules and brokendown frustule biopolymer residues.

Subsequently, 5 ml, 52% HF was added to the frustules in a 15 ml plastic centrifugation tube, and the mixture solution was incubated on ice for 1 h. Hydrogen fluoride was then evaporated under an N_2 stream to reduce the volume to dryness. The remaining material was neutralized with 3 ml Tris–HCl (250 m mol L^{-1}, pH 8.0) and followed by centrifugation at 11,000 g for 15 min with 3000 amu Microsep™ centrifugal filter tubes (Milipore). The filtrate was collected and defined as the fraction of digested silica with <3000 amu frustule BF residues. The supernatant (defined as >3000 amu HF soluble BF, e.g., silaffin) was concentrated to 250 μL and rinsed with milli-Q water. The pellet from this step was then washed by a 3 ml, 200 m mol L^{-1} ammonium acetate solution twice with centrifugation at 3000 g for 20 min. The pellet was then resuspended in a 2 ml, 100 m mol L^{-1} ammonium acetate solution and was sonicated for 20 s until the mixture solution appeared homogenized. After ultracentrifuging the mixture solution at 12,000 g for 5 min, the pellet (>3000 amu HF insoluble BF, e.g., cingulin) was collected and freeze dried for later use. Combined BF from all three HF fractions represented frustule-embedded biopolymers.

2.4. Distribution of ^{234}Th, ^{233}Pa, ^{210}Pb, and ^{7}Be in Diatom Cells

Activity concentrations of ^{234}Th, ^{233}Pa, ^{210}Pb, and ^{7}Be were measured by counting the gamma decay energies at 63.5 keV, 312 keV, 46.5 keV, and 477.6 keV, respectively, on a Canberra ultrahigh purity germanium well detector. Cells, frustule pellets (with embedded proteins), and separated biopolymer fractions (AEPS, NAEPS, EDTA, and SDS extractable BF, <3000 amu frustule BF residues, >3000 amu HF soluble and insoluble BF) collected from different experimental steps were all gamma counted for the activities of ^{234}Th, ^{233}Pa, ^{210}Pb, and ^{7}Be. All reported activities were decay and geometry corrected. ^{233}Pa was added in equilibrium with ^{237}Np, whose activities could be found only in the dissolved phase for all samples, supporting the assumption that very little ^{237}Np would adsorb onto particles relevant for the calculation of the decay and ingrowth corrections of ^{233}Pa [*Atwood*, 2013; *Chuang et al.*, 2013].

2.5. Composition Analysis of Biopolymer Fractions

After partitioning different biopolymeric fractions (Figure 1) collected from lab cultures into aliquots for freeze drying, subsamples were analyzed for individual components. Concentrations of total carbohydrate (TCHO) were determined by the TPTZ (2, 4, 6-tripyridyl-s-triazine) method using glucose as the standard and uronic acids (URA) were measured by the metahydroxyphenyl method using glucuronic acid as the standard [*Hung and Santschi*, 2001]. Protein content was determined using a modified Lowry protein assay, using bovine serum albumin as the standard (Pierce, Thermo Scientific). Organic phosphorus content in frustule biopolymers was determined, after acid hydrolysis, using potassium dihydrogen phosphate, KH_2PO_4, as the standard [*Latimer et al.*, 2006; *Strickland and Parsons*, 1972]. Triplicates were carried out for all compositional analyses, and the maximum relative standard deviations were 10%.

2.6. Nuclear Magnetic Resonance (NMR) Spectroscopy

High-resolution magic angle spinning heteronuclear single quantum coherence ^{1}H-^{13}C 2-D NMR was applied to identify the moieties of biopolymers extracted from diatom frustules. A 2-D HSQC-NMR experiment can detect the ^{1}H-^{13}C bonds in an organic structure. Cross peaks in an HSQC spectrum represent the chemical shift of both carbon and proton atoms in a C-H unit, forming a specific pattern as the "molecular fingerprint" of specific classes of compounds. NMR spectra were obtained on a Bruker Avance II 400 MHz NMR spectrometer using Topspin 2.0 software (Bruker-biospin, Billerica, MA). Optimized procedures and settings are listed below: a freeze-dried sample was dissolved in (dimethylsulfoxide) DMSO-d_6 in a dry atmosphere and was transferred to a 4 mm NMR tube for analysis (to prevent a large water peak that is often centered at 3.3 ppm that can obscure sample signals); the sample was then spun at 7 kHz with an angle of 57.4° to the magnetic field. The ^{13}C spectrum was recorded with ^{1}H decoupling, and ^{13}C decoupling was employed during the detection of ^{1}H signals in the HSQC experiment. The spectral width range employed for all the experiments was 0–150 ppm for ^{13}C and 0–10 ppm for ^{1}H. Spectral simulations and manipulation were carried out using Advanced Chemistry Development's (ACD/Labs) Spec Manager (version 9.15) software.

Table 1. Activities (cpm) of Individual Radionuclides ([234]Th, [233]Pa, ^{210}Pb, and [7]Be) and Amounts (μg) of Organic Components (Proteins, Total Carbohydrates, and Uronic Acids) for Different Biopolymeric Fractions (BF) in Diatom Cells

Activities (cpm)	Extracellular BP		Frustule BP	Intracellular BP	
	NAEPS	AEPS		EDTA	SDS
[234]Th	9.34	2.68	6.43	5.53	1.41
[233]Pa	7.94	4.27	12.60	10.53	11.88
[210]Pb	0.41	2.34	5.99	3.89	0.33
[7]Be	0.46	0.39	2.82	2.89	1.17
Amount (μg)					
Proteins	157.1	39.1	15.5	111.0	161.9
TCHO	152.4	24.5	83.8	172.7	41.0
URA	16.5	4.5	30.8	18.2	87.8

3. Results

3.1. Percentage Binding of Radionuclides in Different Biopolymeric Fractions

As shown in Figure 1, individual biopolymeric fractions (BF) responsible for binding different radionuclides, named after their chemical separation method, are used here to differentiate the source of the biopolymers. The radionuclide activities in each collected BF extracted from *P. tricornutum* are summarized in Table 1, including the extracellular, frustule, and intracellular fractions. Combined NAEPS and AEPS fractions represent extracellular biopolymers; the sum of EDTA and SDS extractable fractions represent intracellular biopolymers; and all HF fractions denote the frustule-related biopolymers.

A comparison of radionuclide distributions among these three major biopolymer fractions is shown in Figure 2a–2c. The sum of percentage activities of each radionuclide in extracellular, frustule, and intracellular BF represents 100%. Results showed affinities to different fractions varied among the different radionuclides (Figure 2). In particular, [234]Th showed the highest affinities to extracellular BF (~47%), followed by intracellular BF (27%), and had the lowest affinity to silica and frustules BF (25%); in contrast, about 48% of [233]Pa was found in the intracellular BF and was about evenly distributed in the extracellular and frustule BF (~26% each); ^{210}Pb was also mostly concentrated in the frustules BF (~46%), followed by the intracellular BF (33%) and the extracellular BF (~21%); [7]Be was mainly bound to intracellular BF (~53%) and had ~36% and 11% bound to frustule BF and extracellular BF, respectively.

Amount distributions of proteins, total carbohydrates (TCHO), and uronic acids (URA) for each BF are also summarized in Table 1. Figure 2d shows the relative amounts of three major organic components in each biopolymeric fraction. The sum of percentages of each organic compound in extracellular, frustule, and intracellular BF represents 100%. In general, proteins and TCHO were mainly distributed in both extracellular (40.5% and 37.3%, respectively) and intracellular (56.3% and 45.0%, respectively) BF. Only a small percentage of proteins (3.2%), TCHO (17.7%), and URA (19.5%) were found in frustule BF. However, the percentage of [234]Th, [233]Pa, ^{210}Pb, and [7]Be activities in frustule BF was up to 25.2%, 26.7%, 46.2%, and 36.5%, respectively, indicating the great importance of frustule BF in the binding of different radionuclides.

3.2. Affinity of Biopolymers and Their Components to Radionuclides

As summarized in Table 1, there are activities of four radionuclides for diatom-associated biopolymeric fractions (NAEPS, AEPS, Frustule, EDTA, and SDS, and they are designated as A, B, C, D, and E, respectively); masses of Protein, TCHO, and URA in each fraction (as $m1$, $m2$, and $m3$, respectively). Activity of a given radionuclide in a given fraction is dependent on the mass (m_i) of the component in each fraction and normalized affinity coefficients (D_i) of the radionuclide for the component. Therefore, the mass balance equation for Th in NAEPS fraction could be written as

$$A_{Th(A)} = D_{Th}1 \times m_{1(A)} + D_{Th}2 \times m_{2(A)} + D_{Th}3 \times m_{3(A)}$$

where $D_{Th}1$, $D_{Th}2$, and $D_{Th}3$ are the normalized affinity coefficients of nuclides to protein, TCHO, and URA, respectively. They have the units of activity per unit mass (cpm/μg) of protein, etc. Similar procedures were applied to other four fractions, as well as to other three radionuclides. It ended up with a total of five
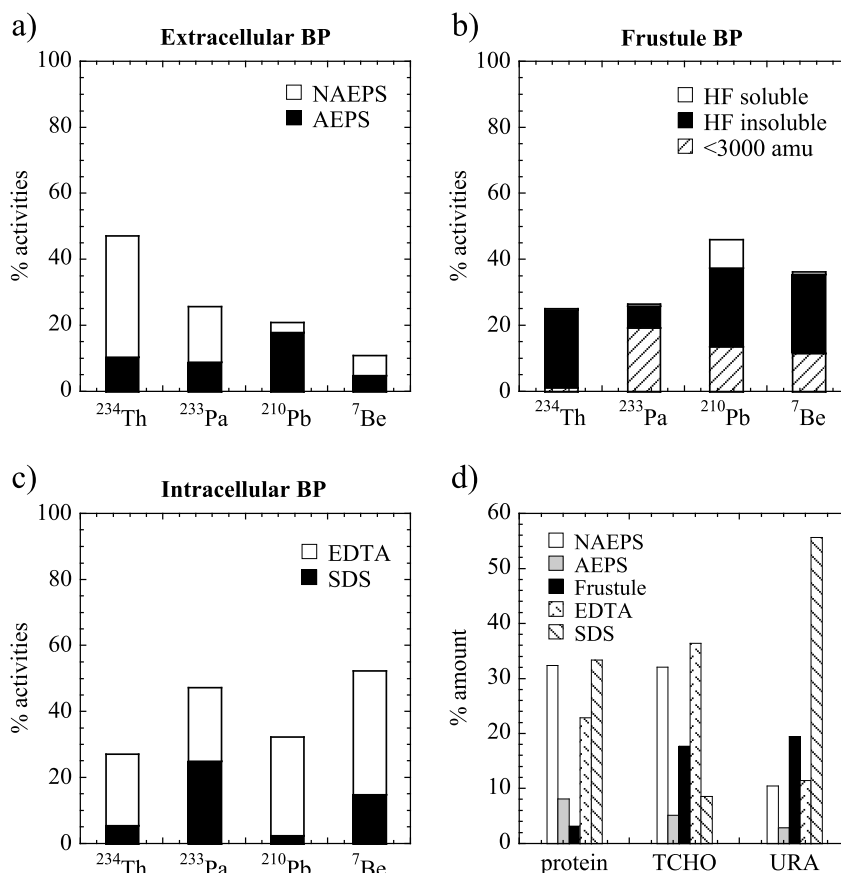
Figure 2. Percentage activities of ^{234}Th, ^{233}Pa, ^{210}Pb, and ^{7}Be in different biopolymer fractions (BF) of diatom cells, including (a) extracellular (NAEPS and AEPS), (b) frustule embedded (>3000 amu HF soluble, >3000 amu HF insoluble, and <3000 amu), and (c) intracellular (EDTA and SDS extractable). (d) Relative amounts of organic components in each biopolymeric fraction. The sum of the percentages of each organic component in extracellular, frustule, and intracellular BF represents 100%.

equations and three unknowns, i.e., $D1$, $D2$, and $D3$, for all tested radionuclides. The overdetermined equations were solved using the nonlinear regression program in IBM SPSS software package. The normalized affinity coefficients of three organic components for radionuclides are defined as ≤1 and ≥0. Result numbers were summarized in Table 2. The higher the coefficient, the higher the affinity of the component to the specific radionuclide is. URA showed overall the highest coefficients among all three measured organic components to all radionuclides, indicating that URA had relatively higher binding affinities to four tested radionuclides.

3.3. Molecular Structures of Frustules Embedded Biopolymers

Results from 2-D HSQC-NMR experiments further revealed the molecular structures of these binding biopolymers extracted from diatom frustules. Due to the complexity of natural samples, even in the liquid-state peak overlap is a major problem in the study of natural organic material by NMR. Thus, a second-dimension NMR technique would be highly beneficial. In general, the spectra can be broken down into four general

Table 2. Normalized Affinity Coefficients of Organic Components ($D1$ for Proteins, $D2$ for Total Carbohydrates, and $D3$ for Uronic Acids) for Individual Radionuclides (^{234}Th, ^{233}Pa, ^{210}Pb, and ^{7}Be)

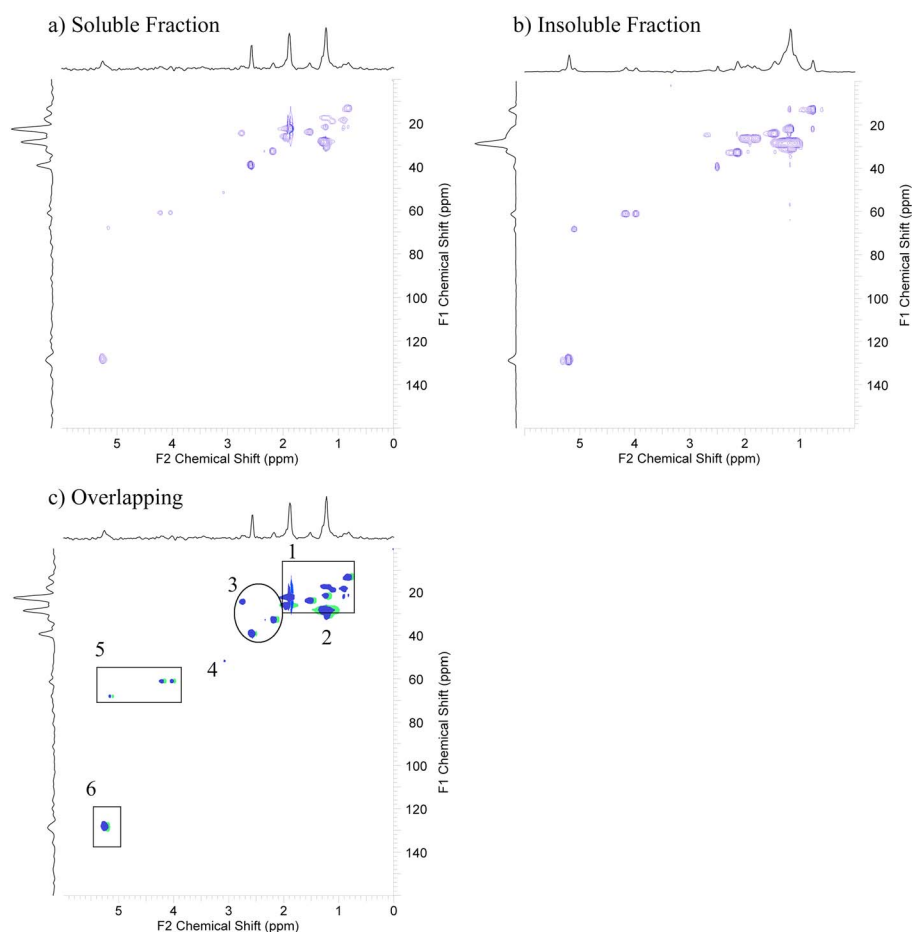|	^{234}Th	^{233}Pa	^{210}Pb	^{7}Be
$D1$ (proteins)	0.000	0.990	0.125	0.000
$D2$ (TCHO)	0.806	1.000	0.000	0.224
$D3$ (URA)	1.000	1.000	0.495	0.611

Figure 3. A 2-D HSQC-NMR spectrum of the diatom frustule biopolymer residues dissolved in DMSO-d_6 from (a) HF soluble fraction and (b) HF insoluble fraction. (c) Overlapping spectra of Figures 3a and 3b (HF soluble and insoluble fractions); assignment of regions: 1. aliphatics; 2. specific methines from intact cyclic terpenoids; 3. carboxyl-rich alicyclic molecule (CRAM); 4. DMSO-d_6 (NMR solvent); 5. amino acid α-proton in peptide chains; 6. nonconjugated double bonds.

groups. These include: the aliphatic region which covers the 1 H region of 0.4 to 3.4 ppm 1 H chemical shift range as well as the 13 C region of 5 to 40 ppm (represented as (0.4–3.4 → 5–40) henceforth), the single heteroatom substituted aliphatic (2.6–5.3 → 40–85), the anomeric (4.2–5.6 → 85–105), and the aromatic (6.0–9.0 → 105–145) regions. Figure 3 shows the 2-D HSQC-NMR spectra of the biopolymer residues from HF soluble (Figure 3a), insoluble (Figure 3b), and the overlapping spectra (Figure 3c) of these two fractions from the diatom frustule. According to *Scheffel et al.* [2011], silaffins are the major proteins in the HF soluble and the <3 kDa fraction. And the term "cingulum" denotes the girdle band region of diatom frustule; hence, the name cingulins is used for the girdle band associated silaffin-like proteins found in the HF insoluble fraction. By overlapping the NMR spectra of soluble fraction with the insoluble fraction, the alignment showed high similarities (Figure 3c). Comparing HSQC spectra of frustule BF with reference biopolymers (protein: albumin bovine serum, carbohydrate: amylopectin) in *Sambrook et al.* [1989], there is a good agreement between the signatures observed from frustule BF (Figures 3a and 3b) and the pattern produced by proteins, and partially by polysaccharides. Five major functional groups were identified from these two frustule BF: aliphatics, specific methines from intact cyclic terpenoids, carboxyl-rich alicyclic molecules (CRAM), methylene and methane from carbohydrates/amino acid α-protons in peptide chains and nonconjugated double bonds. Detailed assignments for these major structural units within corresponding chemical shift ranges are given in Table 3. The phosphate signal observed by NMR was also confirmed by a spectrophotometry method, after separation, showing comparable levels of phosphate in both HF soluble and insoluble fractions. Thus, frustule biopolymers are mainly composed of carboxyl-rich, aliphatic-phosphoprotein molecules. Notably, no molecular fingerprint of aromatic functional groups

Table 3. Two-dimensional HSQC-NMR Spectral Assignments

	^{1}H (ppm)	^{13}C (ppm)	Example Structures	Assigned Functional Groups
1	0.72–2.09	11.44–33.06		aliphatics
2	1.14–1.21	33.69–40.50		Specific methines from intact cyclic terpenoids
3	2.07–2.22	31.07–34.57		CRAM (carboxyl-rich alicyclic molecule)
4	2.47–2.53	37.99–40.85		DMSO (Dimethylsulfoxide, NMR solvent)
5	3.94–5.14	59.71–69.56		Methylene and methine from carbohydrates; amino acid α-protons in peptide chains
6	5.14–5.33	126.1–130.71		Nonconjugated double bonds

was found in the HF-insoluble biopolymeric fraction. Nonetheless, the HSQC experiment detects only ^{1}H attached to ^{13}C and exchangeable protons (OH, NH, etc.) that are detected in the ^{1}H spectrum cannot be observed.

4. Discussion

Opal is known to be a major component in the oceanic particle flux, which can account for up to 52% of the particulate organic carbon (POC) flux in the western North Pacific [*Hayes et al.*, 2014; *Otosaka and Noriki*, 2005]. The surface characteristics of the adsorbate determine the nature of bonding between adsorbate and adsorbent. In *Parida et al.* [2006], the adsorption of organic molecules on the silica surface was evaluated as the first step. Since the surface is already covered by organic macromolecules essential to the functioning of the diatoms, the adsorbate (Th, Pa, Pb, and Be here) would directly bind to the more strongly binding macromolecules rather than to the relatively weak hydroxyl groups on the silica surface. Scanning electron microscope (SEM) pictures in *Tesson and Hildebrand* [2013] showed that the valve proximal surface was covered by a thin layer of organic matrix on the silica frustule of diatoms, which remained present even after SDS cleaning. The absence of an organic phase on cleaned frustules could only be observed by SEM after diatom cells underwent extensive washing and cleaning with high concentrations of strong acids, e.g., concentrated

sulfuric acid and KNO_3. The surface of biogenic silica (i.e., opal) collected from the field would be expected to be covered by biopolymers, e.g., EPS and other frustule biopolymers, which are essential for their growth and functioning. Thus, a layer of biopolymers covering the silica surface is most likely the actual binding phase for any adsorbent including radionuclides. While diatom species could vary between ocean basins and no single species can be representative for the entire ocean diatom community, *Phaeodactylum tricornutum* is both a tychopelagic and estuarine species. *P. tricornutum* is a widely used species and it is frequently chosen for EPS work [e.g., *Abdullahi et al.*, 2006, *Guzmán-Murillo et al.*, 2007, *Chuang et al.*, 2014]. The genome sequence of the pennate diatom *P. tricornutum* was the second diatom genome to be sequenced, after the centric diatom *Thalassiosira pseudonana*. Most importantly, this species was chosen because of its pleiomorphism, with the existence of three morphotypes: oval, fusiform, and triradiate. We have used *P. tricornutum* as a model diatom to study the role of diatom frustules and its related biopolymers on radionuclides adsorption and absorption [*Chuang et al.*, 2014]. Due to the different nature and binding properties of these biopolymers, their affinities to the different radionuclides may vary. This can explain the observed and seemingly contradictory preferential scavenging and fractionation of the different radionuclides with particles from different origins [*Chase and Anderson*, 2004; *Luo and Ku*, 2004], as well as the absence of a significant correlation between bulk organic carbon content and radionuclide flux [*Chase et al.*, 2002; *Chuang et al.*, 2013]. In this work, statistical results (Table 2) further indicate that URA had the highest affinity to tested radionuclides among all tested organic molecules. It is consistent with the findings from the analysis of the combined data sets from the oligotrophic ocean that URA (or acid polysaccharide) content can be used to predict the ^{234}Th flux [*Guo et al.*, 2002b; *Santschi et al.*, 2003; *Xu et al.*, 2011]

As also shown in Figure 2, most Pa, Pb, or Be were associated in the frustules and intracellular biopolymers (Figures 2b and 2c), whereas Th was mostly bound to NAEPS (Figure 2a). Thus, different ratios of these biomolecules could be the main factor controlling preferential scavenging of Pa, Pb, and Be over Th by opal as observed in the field [*Chase et al.*, 2002] and laboratory studies [*Chuang et al.*, 2014; *Guo et al.*, 2002a; *Yang et al.*, 2013], in addition to redox active moieties.

Effects of particle composition on the ability to use individual radionuclides as tracers are well documented in previous studies [*Friedrich and Rutgers van der Loeff*, 2002; *Guo et al.*, 2002a; *Luo and Ku*, 1999]. Radionuclide pairs are also used as tracers to identify specific particle-related phenomena. This includes the use of ^{231}Pa/^{230}Th as a proxy for particle flux and productivity [*Siddall et al.*, 2005; *Walter et al.*, 1997], ^{234}Th$_{xs}$/^{7}Be as a tracer of particle dynamics and sediment transport in a partially mixed estuary [*Feng et al.*, 1999a; *Feng et al.*, 1999b; *Baskaran and Santschi*, 1993; *Santschi et al.*, 1979], and ^{7}Be/^{210}Pb$_{xs}$ as a tracer to identify sediment sources and ages of particles [*Matisoff et al.*, 2005].

Given that ^{231}Pa is generally less efficiently scavenged onto particles than ^{230}Th and is therefore more available to be transported long distances via advection and diffusion before it reaches the ocean sediment, the ^{231}Pa/^{230}Th activity ratio is being used as an important proxy in paleoceanographic studies for boundary scavenging and ocean circulation. However, the particle types that are responsible for fractionating the radionuclides' ratio, e.g., ^{231}Pa/^{230}Th, in the ocean are still being debated [*Li*, 2005; *Scholten et al.*, 2005; *Siddall et al.*, 2005]. In *Siddall et al.* [2005], it was concluded that the lithogenic flux is unimportant for ^{231}Pa/^{230}Th ratios, while the presence of $CaCO_3$ (for Th) or opal (for Pa) were proposed to be the main factors controlling the preferential scavenging between ^{231}Pa and ^{230}Th in the ocean [*Chase et al.*, 2002]. Results from controlled laboratory experiments using biogenic and mineral particles added further insights [*Chuang et al.*, 2014; *Lin et al.*, 2014; *Roberts et al.*, 2009]. Any difference between these radionuclides likely reflects variations of the associated biopolymers from different particles and their origins. In *Hayes et al.* [2014], they concluded that new surface sediment (Pa/Th)$_{xs}$ data from the subarctic Pacific display a clear sensitivity to opal scavenging. A further assessment of the role of opal itself and its associated biopolymers on the scavenging of radionuclides is undoubtedly important. In addition, these authors observed that scavenging of ^{231}Pa is additionally sensitive to the total particle flux and the abundance of particulate MnO_2. This might have resulted from a redox transformation of Pa to become more strongly adsorbed to the particle in the reduced state [*Roberts et al.*, 2009; *Chuang et al.*, 2013].

In *Friedrich and Rutgers van der Loeff* [2002], preferential adsorption of ^{210}Pb compared to ^{210}Po onto siliceous frustules was observed. However, with pure SiO_2 particles and acid-cleaned diatom frustules, no significant difference between absorption of ^{210}Pb and ^{210}Po could be found in controlled laboratory experiments

[*Chuang et al.*, 2014]. The preferential adsorption of ^{210}Pb over ^{210}Po was only evident in the treatment with noncleaned whole diatom cells. In Figure 2b, Pb had the highest percentage to frustules BF among all tested radionuclides, indicating that the main binding phases of ^{210}Pb in the siliceous frustules were chelating frustule-associated biopolymers.

5. Conclusions

Global Ocean Flux Studies (e.g., GEOSECS, JGOFS, GEOTRACES, and Middle Atlantic Bight Studies) have applied natural radionuclides as tracers or proxies of particulate flux in the oceans for decades. However, only few studies have attempted to understand the molecular mechanism to support the precise use of these tracers in light of the importance of differential tracer uptake on biogenic-silica-associated biopolymers that help to control the marine carbon flux. It is thus very important to know which components of particles, e.g., minerals or organic matter, the radionuclides are sorbing and thus tracing, thus providing for more accurate predictions of carbon sequestration in the ocean. This work, for the first time, comprehensively examined the carrier phases of ^{234}Th, ^{233}Pa, ^{210}Pb, and ^{7}Be incubated together with cultured diatom cells and determined the chemical characteristics of their radionuclide-binding moieties at the molecular level. In the ternary sorption system (biogenic silica-biopolymers-radionuclides), we provided solid evidence that it is not the mineral phase, biogenic silica but the biopolymers associated with the mineral phase (biogenic SiO$_2$ here) that are providing the strong binding sites for the different radionuclides. This also accounts for the majority of the binding of the selected radionuclides [*Chuang et al.*, 2014]. In this work, we provided further evidence for these so far mostly ignored metal-organic biopolymers. The preferential scavenging of different radionuclides observed in the field and laboratory studies are thus controlled by the different biopolymers from different particle origins, as well as the ballasting minerals opal, calcite, or lithogenic particles, all covered by EPS. Therefore, it is not surprising that the bulk POC content was not found to be a very good proxy to predict the radionuclide scavenging. As a consequence, controversies continue to exist as to the nature of the different carrier phases, so far mostly inorganic, that had been proposed in different studies.

Moreover, it has been estimated that substantial cell death by lysis may exceed 50% of phytoplankton growth in field phytoplankton populations [*Bidle and Falkowski*, 2004]. There are some distinct morphological changes and biogeochemical pathways that develop during the programmed cell death of phytoplankton, leading to the lysis of the cell [*Berman-Frank et al.*, 2004; *Bidle and Falkowski*, 2004]. In earlier studies, researchers reported that cell lysis played an important role in phytoplankton bloom termination [*Baldi et al.*, 1997]. Recently, *Armbrecht et al.* [2014] reported that intracellular material has been released after cell lysis at high cell densities and the released particulate polysaccharides have been correlated to massive mucilage events. The cell lysis process may happen mainly in the surface ocean especially during bloom events, but phytoplankton can sink quickly when it is stressed, so it is possible that the release of intracellular substances may happen along with sedimentation path of bloom plankton [*Bienfang et al.*, 1982; *Bienfang and Harrison*, 1984]. Although these radionuclides are not essential elements for algae, they would still be taken up inadvertently. When the algae die, the radionuclides could be recycled back to the surrounding environment during cell lysis. Therefore, the effects of inner-cellular fraction on the scavenging and fractionation of radionuclides cannot be ignored.

The differences between the affinities of ^{234}Th, ^{233}Pa, ^{210}Pb, and ^{7}Be for different organic components were clearly evident in this study. Due to the compositional variability in different biopolymeric fractions, radionuclides were enriched differently in different organic fractions extracted from the diatoms. In the extracellular BF of the diatoms, the radionuclide-binding macromolecules contained mainly URA-binding moieties. The frustule BF, which is the most likely fraction in the sinking particle flux that is preserved in the historical record, could have great importance for the fate of these radionuclides. Our results from statistical analyses, 2-D HSQC-NMR and spectrophotometric determinations indicate that frustule biopolymers are mainly composed of carboxyl-rich, aliphatic-phosphoproteins that are providing strong binding sites for some of the radionuclides.

Overall, the interactions of different biopolymers with particle surfaces are likely exerting ultimate control of the scavenging of radionuclides in the ocean. However, the work here has shown that it would be unrealistic to assume one single compound to be responsible for binding a single or any radionuclide. Rather, a number of compounds act in concert to bind and incorporate the different radioactive metals to the diatom surface. Thus, our extensive and comprehensive molecular-level analyses of radionuclide

carrier macromolecules should help to resolve some of the seemingly controversial observations on the scavenging and fractionation of radionuclides in the ocean. A better understanding of the main controlling factors of the fractionation of radionuclides should also help in the use of the appropriate radioactive tracers in paleoceanographic reconstructions.

References

Abdullahi, A. S., G. J. C. Underwood, and M. R. Gretz (2006), Extracellular matrix assembly in diatoms (bacillariophyceae). V. Environmental effects on polysaccharide synthesis in the model diatom *Phaeodactylum Tricornutum*, *J. Phycol.*, *42*(2), 363–378.

Alvarado Quiroz, N. G., C.-C. Hung, and P. H. Santschi (2006), Binding of thorium(IV) to carboxylate, phosphate and sulfate functional groups from marine exopolymeric substances (EPS), *Mar. Chem.*, *100*(3–4), 337–353.

Anderson, R. F., M. P. Bacon, and P. G. Brewer (1983), Removal of ^{230}Th and ^{231}Pa at ocean margins, *Earth Planet. Sci. Lett.*, *66*(C), 73–90.

Armbrecht, L. H., V. Smetacek, P. Assmy, and C. Klaas (2014), Cell death and aggregate formation in the giant diatom *Coscinodiscus wailesii* (Gran & Angst, 1931), *J. Exp. Mar. Biol. Ecol.*, *452*, 31–39.

Atwood, D. A. (2013), *Radionuclides in the Environment*, Wiley, New York.

Bacon, M. P., D. W. Spencer, and P. G. Brewer (1976), ^{210}Pb/^{226}Ra and ^{210}Po/^{210}Pb disequilibria in seawater and suspended particulate matter, *Earth Planet. Sci. Lett.*, *32*(2), 277–296.

Baldi, F., A. Minacci, A. Saliot, L. Mejanelle, P. Mozetic, V. Turk, and A. Malej (1997), Cell lysis and release of particu-late polysaccharides in extensive marine mucilage assessed by lipid biomarkers and molecular probes, *Mar. Ecol. Prog. Ser.*, *153*, 45–57.

Baskaran, M., and P. H. Santschi (1993), The role of particles and colloids in the transport of radionuclides in coastal environments of Texas, *Mar. Chem.*, *43*, 95–114.

Berman-Frank, I., K. D. Bidle, L. Haramaty, and P. G. Falkowski (2004), The demise of the marine cyanobacterium, *Trichodesmium* spp., via an autocatalyzed cell death pathway, *Limnol. Oceanogr.*, *49*, 997–1005.

Bidle, K. D., and P. G. Falkowski (2004), Cell death in planktonic, photosynthetic microorganisms, *Nat. Rev. Microbiol.*, *2*, 643–655.

Bienfang, P. K., and P. J. Harrison (1984), Sinking-rate response of natural assemblages of temperate and subtropical phytoplankton to nutrient depletion, *Mar. Biol.*, *83*, 293–300.

Bienfang, P. K., P. J. Harrison, and L. M. Quarmby (1982), Sinking rate response to depletion of nitrate, phosphate and silicate in four marine diatoms, *Mar. Biol.*, *67*, 295–302.

Buesseler, K. O. (1998), The decoupling of production and particulate export in the surface ocean, *Global Biogeochem. Cycles*, *12*(2), 297–310, doi:10.1029/97GB03366.

Burnett, W. C., D. R. Corbett, M. Schultz, E. P. Horwitz, R. Chiarizia, M. Dietz, A. Thakkar, and M. Fern (1997), Pre-concentration of actinide elements from soils and large volume water samples using extraction chromatography, *J. Radioanal. Nucl. Chem.*, *226*(1–2), 121–127.

Chase, Z., and R. F. Anderson (2004), Comment on "On the importance of opal, carbonate, and lithogenic clays in scavenging and fractionating ^{230}Th, ^{231}Pa and ^{10}Be in the ocean" by S. Luo and T.-L Ku, *Earth Planet. Sci. Lett.*, *220*(1–2), 213–222.

Chase, Z., R. F. Anderson, M. Q. Fleisher, and P. W. Kubik (2002), The influence of particle composition and particle flux on scavenging of Th, Pa and Be in the ocean, *Earth Planet. Sci. Lett.*, *204*(1–2), 215–229.

Chuang, C.-Y., P. H. Santschi, Y.-F. Ho, M. H. Conte, L. Guo, D. Schumann, M. Ayranov, and Y.-H. Li (2013), Role of biopolymers as major carrier phases of Th, Pa, Pb, Po, and Be radionuclides in settling particles from the Atlantic Ocean, *Mar. Chem.*, *157*, 131–143.

Chuang, C.-Y., P. H. Santschi, Y. Jiang, Y.-F. Ho, A. Quigg, L. D. Guo, M. Ayranov, and D. Schumann (2014), Important role of biomolecules from diatoms in the scavenging of particle reactive radionuclides of thorium, protactinium, lead, polonium, and beryllium, in the ocean: A case study with *Phaeodactylum tricornutum*, *Limnol. Oceanogr.*, *59*(4), 1256–1266.

Chuang, C.-Y., et al. (2015), Binding of Th, Pa, Pb, Po and Be radionuclides to marine colloidal macromolecular organic matter, *Mar. Chem.*, *173*, 320–329.

Cochran, J. K., M. P. Bacon, S. Krishnaswami, and K. K. Turekian (1983), ^{210}Po and ^{210}Pb distributions in the central and eastern Indian-Ocean, *Earth Planet. Sci. Lett.*, *65*(2), 433–452.

Das, S. K., and E. Marsili (2011), Bioinspired metal nanoparticle: synthesis, properties and application, in *Nanomaterials*, edited by M. Rahman, pp. 253–278, In Tech, Europe.

Feng, H., J. K. Cochran, and D. J. Hirschberg (1999a), ^{234}Th and ^{7}Be as tracers for transport and sources of particle-associated contaminants in the Hudson River estuary, *Sci. Total Environ.*, *237–238*, 401–418.

Feng, H., J. K. Cochran, and D. J. Hirschberg (1999b), Th-234 and Be-7 as tracers for the transport and dynamics of suspended particles in a partially mixed estuary, *Geochim. Cosmochim. Acta*, *63*(17), 2487–2505.

Friedrich, J., and M. M. Rutgers van der Loeff (2002), A two-tracer (^{210}Po-^{234}Th) approach to distinguish organic carbon and biogenic silica export flux in the Antarctic circumpolar current, *Deep Sea Res., Part I*, *49*(1), 101–120.

Guo, L. D., P. H. Santschi, M. Baskaran, and A. Zindler (1995), Distribution of dissolved and particulate ^{230}Th and ^{232}Th in seawater from the Gulf of Mexico and off Cape Hatteras as measured by SIMS, *Earth Planet. Sci. Lett.*, *133*(1–2), 117–128.

Guo, L. D., M. Chen, and C. Gueguen (2002a), Control of Pa/Th ratio by particulate chemical composition, *Geophys. Res. Lett.*, *29*(20), 1960, doi:10.1029/2002GL015543.

Guo, L. D., C. C. Hung, P. H. Santschi, and I. D. Walsh (2002b), ^{234}Th scavenging and its relationship to acid polysaccharide abundance in the Gulf of Mexico, *Mar. Chem.*, *78*(2–3), 103–119.

Guzmán-Murillo, M., C. López-Bolaños, T. Ledesma-Verdejo, G. Roldan-Libenson, M. Cadena-Roa, and F. Ascencio (2007), Effects of fertilizer-based culture media on the production of exocellular polysaccharides and cellular superoxide dismutase by Phaeodactylum tricornutum (Bohlin), *J. Appl. Phycol.*, *19*(1), 33–41.

Hayes, C. T., R. F. Anderson, M. Q. Fleisher, S. Serno, G. Winckler, and R. Gersonde (2014), Biogeography in ^{231}Pa/^{230}Th ratios and a balanced ^{231}Pa budget for the Pacific Ocean, *Earth Planet. Sci. Lett.*, *391*, 307–318.

Hung, C. C., and P. H. Santschi (2001), Spectrophotometric determination of total uronic acids in seawater using cation-exchange separation and pre-concentration by lyophilization, *Anal. Chim. Acta*, *427*(1), 111–117.

Kröger, N., and N. Poulsen (2008), Diatoms—From cell wall biogenesis to nanotechnology, *Annu. Rev. Genet.*, *42*(1), 83–107.

Kröger, N., R. Deutzmann, and M. Sumper (1999), Polycationic peptides from diatom biosilica that direct silica nanosphere formation, *Science*, *286*(5442), 1129–1132.

Kröger, N., S. Lorenz, E. Brunner, and M. Sumper (2002), Self-assembly of highly phosphorylated silaffins and their function in biosilica morphogenesis, *Science*, *298*(5593), 584–586.

Latimer, J. C., G. M. Filippelli, I. Hendy, and D. R. Newkirk (2006), Opal-associated particulate phosphorus: Implications for the marine P cycle, *Geochim. Cosmochim. Acta*, *70*(15), 3843–3854.

Li, Y.-H. (2005), Controversy over the relationship between major components of sediment-trap materials and the bulk distribution coefficients of ^{230}Th, ^{231}Pa, and ^{10}Be, *Earth Planet. Sci. Lett.*, *233*(1–2), 1–7.

Li, Y.-H., H. W. Feely, and P. H. Santschi (1979), Th-228 radioactive Ra-228 radioactive disequilibrium in the New-York Bight and its implications for coastal pollution, *Earth Planet. Sci. Lett.*, *42*(1), 13–26.

Lin, P., L. Guo, and M. Chen (2014), Adsorption and fractionation of thorium and protactinium on nanoparticles in seawater, *Mar. Chem.*, *162*, 50–59.

Luo, S., and T. L. Ku (1999), Oceanic ^{231}Pa/^{230}Th ratio influenced by particle composition and remineralization, *Earth Planet. Sci. Lett.*, *167*(3–4), 183–195.

Luo, S., and T. L. Ku (2004), On the importance of opal, carbonate, and lithogenic clays in scavenging and fractionating ^{230}Th, ^{231}Pa and ^{10}Be in the ocean, *Earth Planet. Sci. Lett.*, *220*(1–2), 201–211.

Matisoff, G., C. G. Wilson, and P. J. Whiting (2005), The ^{7}Be/^{210}Pb$_{xs}$ ratio as an indicator of suspended sediment age or fraction new sediment in suspension, *Earth Surf. Processes Landforms*, *30*(9), 1191–1201.

Mort, A. J., and D. T. A. Lamport (1977), Anhydrous hydrogen fluoride deglycosylates glycoproteins, *Anal. Biochem.*, *82*(2), 289–309.

Nelson, D. M., P. Treguer, M. A. Brzezinski, A. Leynaert, and B. Queguiner (1995), Production and dissolution of biogenic silica in the ocean— Revised global estimates, comparison with regional data and relationship to biogenic sedimentation, *Global Biogeochem. Cycles*, *9*(3), 359–372, doi:10.1029/95GB01070.

Otosaka, S., and S. Noriki (2005), Relationship between composition of settling particles and organic carbon flux in the western North Pacific and the Japan Sea, *J. Oceanogr.*, *61*(1), 25–40.

Parida, S. K., S. Dash, S. Patel, and B. K. Mishra (2006), Adsorption of organic molecules on silica surface, *Adv. Colloid Interface Sci.*, *121*(1–3), 77–110.

Quigley, M. S., P. H. Santschi, C. C. Hung, L. D. Guo, and B. D. Honeyman (2002), Importance of acid polysaccharides for ^{234}Th complexation to marine organic matter, *Limnol. Oceanogr.*, *47*(2), 367–377.

Richardson, T. L., and G. A. Jackson (2007), Small phytoplankton and carbon export from the surface ocean, *Science*, *315*(5813), 838–840.

Roberts, K. A., C. Xu, C. C. Hung, M. H. Conte, and P. H. Santschi (2009), Scavenging and fractionation of thorium vs. protactinium in the ocean, as determined from particle-water partitioning experiments with sediment trap material from the Gulf of Mexico and Sargasso Sea, *Earth Planet. Sci. Lett.*, *286*(1–2), 131–138.

Sambrook, J., E. F. Fritsch, T. Maniatis, and C. Nolan (1989), *Molecular Cloning: A Laboratory Manual*, Cold Spring Harbor Laboratory, New York.

Santschi, P. H. (1984), Particle-flux and trace-metal residence time in natural-waters, *Limnol. Oceanogr.*, *29*(5), 1100–1108.

Santschi, P. H., Y. H. Li, and J. Bell (1979), Natural radionuclides in the water of Narragansett Bay, *Earth Planet. Sci. Lett.*, *45*(1), 201–213.

Santschi, P. H., D. Adler, M. Amdurer, Y. H. Li, and J. J. Bell (1980), Thorium isotopes as analogs for particle-reactive pollutants in coastal marine environments, *Earth Planet. Sci. Lett.*, *47*(3), 327–335.

Santschi, P. H., C. C. Hung, G. Schultz, N. Alvarado-Quiroz, L. Guo, J. Pinckney, and I. Walsh (2003), Control of acid polysaccharide production and ^{234}Th and POC export fluxes by marine organisms, *Geophys. Res. Lett.*, *30*(2), 16–11, doi:10.1029/2002GL016046.

Santschi, P. H., J. W. Murray, M. Baskaran, C. R. Benitez-Nelson, L. D. Guo, C. C. Hung, C. Lamborg, S. B. Moran, U. Passow, and M. Roy-Barman (2006), Thorium speciation in seawater, *Mar. Chem.*, *100*(3–4), 250–268.

Scheffel, A., N. Poulsen, S. Shian, and N. Kröger (2011), Nanopatterned protein microrings from a diatom that direct silica morphogenesis, *Proc. Natl. Acad. Sci. U.S.A.*, *108*, 3175–3180.

Scholten, J. C., et al. (2005), Radionuclide fluxes in the Arabian Sea: The role of particle composition, *Earth Planet. Sci. Lett.*, *230*(3–4), 319–337.

Schumann, D., M. Ayranov, T. Stowasser, L. Gialanella, A. di Leva, M. Romano, and D. Schuermann (2013), Radiochemical separation of ^{7}Be from the cooling water of the neutron spallation source SINQ at PSI, *Radiochim. Acta*, *101*, 509–514.

Siddall, M., G. M. Henderson, N. R. Edwards, M. Frank, S. A. Müller, T. F. Stocker, and F. Joos (2005), ^{231}Pa and ^{230}Th fractionation by ocean transport, biogenic particle flux and particle type, *Earth Planet. Sci. Lett.*, *237*(1–2), 135–155.

Strickland, J. D. H., and T. R. Parsons (1972), *A Practical Handbook of Seawater Analysis*, 2nd ed., Fisheries Research Board of Canada, Ottawa.

Šulcek, Z., and P. Povondra (1989), *Methods of Decomposition in Inorganic Analysis*, CRC Press, Boca Raton, Fla.

Tesson, B., and M. Hildebrand (2013), Characterization and localization of insoluble organic matrices associated with diatom cell walls: Insight into their roles during cell wall formation, *PLoS One*, *8*(4), e61675.

Walter, H. J., M. M. R. van der Loeff, and H. Hoeltzen (1997), Enhanced scavenging of ^{231}Pa relative to ^{230}Th in the south Atlantic south of the Polar front: Implications for the use of the Pa-231/Th-230 ratio as a paleoproductivity proxy, *Earth Planet. Sci. Lett.*, *149*(1–4), 85–100.

Xu, C., et al. (2011), Controls of ^{234}Th removal from the oligotrophic ocean by polyuronic acids and modification by microbial activity, *Mar. Chem.*, *123*(1–4), 111–126.

Yang, W., L. Guo, C.-Y. Chuang, D. Schumann, M. Ayranov, and P. H. Santschi (2013), Adsorption characteristics of ^{210}Pb, ^{210}Po and ^{7}Be onto micro-particle surfaces and the effects of macromolecular organic compounds, *Geochim. Cosmochim. Acta*, *107*, 47–64.